SLAC–PUB–8998
September 2001

Diffraction Dissociation in QCD and Light-Cone Wavefunctions*

Stanley J. Brodsky
Stanford Linear Accelerator Center
Stanford University, Stanford, California 94309
E-mail: sjbth@slac.stanford.edu

Abstract

The diffractive dissociation of a hadron at high energies, by either Coulomb or Pomeron exchange, has a natural description in QCD as the materialization of the projectile's light-cone wavefunctions; in particular, the diffractive dissociation of a meson, baryon, or photon into high transverse momentum jets measures the shape and other features of the projectile's distribution amplitude. Diffractive dissociation can thus test fundamental properties of QCD, including color transparency and intrinsic charm. All of these effects have an impact on exclusive decays of B mesons and the study of CP violation. I also discuss recent work which shows that the structure functions measured in deep inelastic lepton scattering are affected by final-state rescattering, thus modifying their connection to light-cone probability distributions. In particular, the shadowing of nuclear structure functions is due to destructive interference effects from leading-twist diffraction of the virtual photon, physics not included in the nuclear light-cone wavefunctions.

Presented at the Workshop on
9th Blois Workshop On Elastic And Diffractive Scattering
Pruhonice, Prague, Czech Republic
9-15 June 2001

*Work supported by Department of Energy contract DE–AC03–76SF00515.

1 Introduction

The diffractive dissociation of a hadron at high energies, by either Coulomb or Pomeron exchange, can be understood as the materialization of the projectile's light-cone wavefunctions; in particular, the diffractive dissociation of a meson, baryon, or photon into high transverse momentum jets measures the shape and other features of the projectile's distribution amplitude, $\phi(x_i, Q)$, the valence wavefunction which controls high momentum transfer exclusive amplitudes. Diffractive dissociation can also test fundamental properties of QCD, including color transparency and intrinsic charm.

Diffractive dissociation in QCD can be understood as a three-step process:

1. The initial hadron can be decomposed in terms of its quark and gluon constituents in terms of its light-cone Fock-state components. For example, the eigensolution of a negatively-charged meson QCD, projected on its color-singlet $B = 0$, $Q = -1$, $J_z = 0$ eigenstates $\{|n\rangle\}$ of the free Hamiltonian $H_{LC}^{QCD}(g = 0)$ at fixed $\tau = t - z/c$ has the expansion:

$$\left|\Psi; P^+, \vec{P}_\perp, \lambda\right\rangle = \sum_{n\geq 2,\lambda_i} \int \Pi_{i=1}^n \frac{d^2k_{\perp i}dx_i}{\sqrt{x_i}16\pi^3} 16\pi^3 \delta\left(1 - \sum_j^n x_j\right) \delta^{(2)}\left(\sum_\ell^n \vec{k}_{\perp\ell}\right) \left|n; x_iP^+, x_i\vec{P}_\perp + \vec{k}_{\perp i}, \lambda_i\right\rangle \psi_{n/p}(x_i, \vec{k}_{\perp i}, \lambda_i).$$

The light-cone momentum fractions $x_i = k_i^+/P_\pi^+ = (k^0+k_i^z)/(P^0+P^z)$ with $\sum_{i=1}^n x_i = 1$ and $\vec{k}_{\perp i}$ with $\sum_{i=1}^n \vec{k}_{\perp i} = \vec{0}_\perp$ represent the relative momentum coordinates of the QCD constituents independent of the total momentum of the state. The actual physical transverse momenta are $\vec{p}_{\perp i} = x_i\vec{P}_\perp + \vec{k}_{\perp i}$. The λ_i label the light-cone spin S^z projections of the quarks and gluons along the quantization z direction. The physical gluon polarization vectors $\epsilon^\mu(k,\ \lambda = \pm 1)$ are specified in light-cone gauge by the conditions $k \cdot \epsilon = 0,\ \eta \cdot \epsilon = \epsilon^+ = 0$. The parton degrees of freedom are thus all physical; there are no ghost or negative metric states. Remarkably, the light-cone Fock wavefunctions $\psi_{n/p}(x_i, \vec{k}_{\perp i}, \lambda_i)$ are independent of the proton's momentum $P^+ = P^0 + P^z$, and $P_\perp$. The wavefunctions represent the ensembles of states possible when the hadron is intercepted by a light-front at fixed $\tau = t + z/c$. The light-cone representation thus provide a frame-independent, quantum-mechanical representation of the incoming hadron at the amplitude level, capable of encoding its multi-quark, hidden-color and gluon momentum, helicity, and flavor correlations in the form of universal process-independent hadron wavefunctions.

Progress in measuring the basic parameters of electroweak interactions and CP violation will require a quantitative understanding of the dynamics and phase structure of B decays at the amplitude level. The light-cone Fock representation is specially advantageous in the study of exclusive B decays. For example, Dae Sung Hwang [1] and I have derived an exact frame-independent representation of decay matrix elements such as $B \to D\ell\overline{\nu}$ from the overlap of $n' = n$ parton-number conserving wavefunc-

tions and the overlap of wavefunctions with $n' = n - 2$ from the annihilation of a quark-antiquark pair in the initial wavefunction.

2. In the second step, the incoming hadron is resolved by Pomeron or Odderon (multi-gluon) exchange with the target or by Coulomb dissociation. The exchanged interaction has to supply sufficient momentum transfer q^μ to put the diffracted state X on shell. Light-cone energy conservation requires $q^- = (m_X^2 - m_\pi^2)/P_\pi^+$, where m_X is the invariant mass of X. In a heavy target rest system, the longitudinal momentum transfer is $q^z = (m_X^2 - m_\pi^2)/E_{\pi\mathrm{lab}}$. Thus the momentum transfer $t = q^2$ to the target can be sufficiently small so that the target remains intact.

In perturbative QCD, the pomeron is generally be represented as multiple gluon exchange between the target and projectile. Effectively this interaction occurs over a short light-cone time interval, and thus like photon exchange, the perturbative QCD pomeron can be effectively represented as a local operator. This description is believed to be applicable when the pomeron has to resolve compact states and is the basis for the terminology "hard pomeron". The BFKL formalism generalizes the perturbative QCD treatment by an all-orders perturbative resummation, generating a pomeron with a fixed Regge intercept $\alpha_P(0)$. Next to leading order calculations with BLM scale fixing leads to a predicted intercept $\alpha_P(0) \simeq 0.4$ [2]. However, when the exchange interactions are soft, a multiperipheral description in terms of meson ladders may dominate the physics. This is the basis for the two-component pomeron model of Donachie and Landshoff [3].

Consider a collinear frame where the incident momentum P_π^+ is large and $s = (p_\pi + p_{\mathrm{target}})^2 \simeq p_\pi^+ p_{\mathrm{target}}^-$. The matrix element of an exchanged gluon with momentum q_i between the projectile and an intermediate state $|N\rangle$ is dominated by the "plus current": $\left\langle \pi | j^+(0) \exp(i\frac{1}{2} q_i^+ x^- - i q_{\perp i} \cdot x_\perp | N \right\rangle$. Note that the coherent sum of couplings of an exchanged gluon to the pion system vanishes when its momentum is small compared to the characteristic momentum scales in the projectile light-cone wavefunction: $q^{\perp i} \Delta x_\perp \ll 1$ and $q_i^+ \Delta x^- \ll 1$. The destructive interference of the gauge couplings to the constituents of the projectile follows simply from the fact that the color charge operator has zero matrix element between distinct eigenstates of the QCD Hamiltonian: $\langle A|Q|B\rangle \equiv \int d^2x_\perp dx^- \langle A|j^+(0)|B\rangle = 0$ [4]. At high energies the change in k_i^+ of the constituents can be ignored, so that Fock states of a hadron with small transverse size interact weakly even in a nuclear target because of their small dipole moment. This is the basis of "color transparency" in perturbative QCD [5, 6]. To a good approximation the sum of couplings to the constituents of the projectile can be represented as a derivative with respect to transverse momentum. Thus photon exchange measures a weighted sum of tranverse derivatives $\partial_{k_\perp} \psi_n(x_i, k_{\perp_i}, \lambda_i)$, and two-gluon exchange measures the second transverse partial derivative [7].

3. The final step is the hadronization of the n constituents of the projectile Fock state into final state hadrons. Since q_i^+ is small, the number of partons in the initial Fock state and the final state hadrons are unchanged. Their coalescence is thus governed by the convolution of initial and final-state Fock state wavefunctions. In

the case of states with high $k_\perp$, the final state will hadronize into jets, each reflecting the respective x_i of the Fock state constituents. In the case of higher Fock states with intrinsic sea quarks such as an extra $c\bar{c}$ pair (intrinsic charm), one will observe leading J/ψ or open charm hadrons in the projectile fragmentation region; *i.e.*, the hadron's fragments will tend to have the same rapidity as that of the projectile.

For example, diffractive multi-jet production in heavy nuclei provides a novel way to measure the shape of the LC Fock state wavefunctions and test color transparency. Consider the reaction [6, 8, 9] $\pi A \to \mathrm{Jet}_1 + \mathrm{Jet}_2 + A'$ at high energy where the nucleus A' is left intact in its ground state. The transverse momenta of the jets balance so that $\vec{k}_{\perp i} + \vec{k}_{\perp 2} = \vec{q}_\perp < R^{-1}{}_A$. The light-front longitudinal momentum fractions also need to add to $x_1 + x_2 \sim 1$ so that $\Delta p_L < R_A^{-1}$. The process can then occur coherently in the nucleus. Because of color transparency, the valence wavefunction of the pion with small impact separation, will penetrate the nucleus with minimal interactions, diffracting into jet pairs [6]. The $x_1 = x$, $x_2 = 1 - x$ dependence of the di-jet distributions will thus reflect the shape of the pion valence light-front wavefunction in x; similarly, the $\vec{k}_{\perp 1} - \vec{k}_{\perp 2}$ relative transverse momenta of the jets gives key information on the second derivative of the underlying shape of the valence pion wavefunction [8, 9, 7]. The diffractive nuclear amplitude extrapolated to $t = 0$ should be linear in nuclear number A if color transparency is correct. The integrated diffractive rate should then scale as $A^2/R_A^2 \sim A^{4/3}$.

The results of a diffractive dijet dissociation experiment of this type E791 at Fermilab using 500 GeV incident pions on nuclear targets [10] appear to be consistent with color transparency. The measured longitudinal momentum distribution of the jets [11] is consistent with a pion light-cone wavefunction of the pion with the shape of the asymptotic distribution amplitude, $\phi_\pi^{\mathrm{asympt}}(x) = \sqrt{3} f_\pi x(1-x)$. Data from CLEO [12] for the $\gamma\gamma^* \to \pi^0$ transition form factor also favor a form for the pion distribution amplitude close to the asymptotic solution to the perturbative QCD evolution equation [13].

The interpretation of the diffractive dijet processes as measures of the hadron distribution amplitudes has recently been questioned by Braun *et al.* [14] and by Chernyak [15] who have calculated the hard scattering amplitude for such processes at next-to-leading order. However, these analyses neglect the integration over the transverse momentum of the valence quarks and thus miss the logarithmic ordering which is required for factorization of the distribution amplitude and color-filtering in nuclear targets.

As noted above, the diffractive dissociation of a hadron or nucleus can also occur via the Coulomb dissociation of a beam particle on an electron beam (*e.g.* at HERA or eRHIC) or on the strong Coulomb field of a heavy nucleus (*e.g.* at RHIC or nuclear collisions at the LHC) [7]. The amplitude for Coulomb exchange at small momentum transfer is proportional to the first derivative $\sum_i e_i \frac{\partial}{\vec{k}_{Ti}} \psi$ of the light-front wavefunction, summed over the charged constituents. The Coulomb exchange reactions fall off less fast at high transverse momentum compared to pomeron exchange reactions since

the light-front wavefunction is effective differentiated twice in two-gluon exchange reactions.

It will also be interesting to study diffractive tri-jet production using proton beams $pA \to \mathrm{Jet}_1 + \mathrm{Jet}_2 + \mathrm{Jet}_3 + A'$ to determine the fundamental shape of the 3-quark structure of the valence light-front wavefunction of the nucleon at small transverse separation [8]. For example, consider the Coulomb dissociation of a high energy proton at HERA. The proton can dissociate into three jets corresponding to the three-quark structure of the valence light-front wavefunction. We can demand that the produced hadrons all fall outside an opening angle θ in the proton's fragmentation region. Effectively all of the light-front momentum $\sum_j x_j \simeq 1$ of the proton's fragments will thus be produced outside an "exclusion cone". This then limits the invariant mass of the contributing Fock state $M_n^2 > \Lambda^2 = P^{+2} \sin^2\theta/4$ from below, so that perturbative QCD counting rules can predict the fall-off in the jet system invariant mass M. The segmentation of the forward detector in azimuthal angle ϕ can be used to identify structure and correlations associated with the three-quark light-front wavefunction [7]. One can use also measure the dijet structure of real and virtual photons beams $\gamma^* A \to \mathrm{Jet}_1 + \mathrm{Jet}_2 + A'$ to measure the shape of the light-front wavefunction for transversely-polarized and longitudinally-polarized virtual photons. Such experiments will open up a direct window on the amplitude structure of hadrons at short distances. The light-front formalism is also applicable to the description of nuclei in terms of their nucleonic and mesonic degrees of freedom [16, 17]. Self-resolving diffractive jet reactions in high energy electron-nucleus collisions and hadron-nucleus collisions at moderate momentum transfers can thus be used to resolve the light-front wavefunctions of nuclei.

2 Heavy Quark Fluctuations in Diffractive Dissociation

Since a hadronic wavefunction describes states off of the light-cone energy shell, there is a finite probability of the projectile having fluctuations containing extra quark-antiquark pairs, such as intrinsic strangeness charm, and bottom. In contrast to the quark pairs arising from gluon splitting, intrinsic quarks are multiply-connected to the valence quarks and are thus part of the dynamics of the hadron. Recently Franz, Polyakov, and Goeke have analyzed the properties of the intrinsic heavy-quark fluctuations in hadrons using the operator-product expansion [18]. For example, the light-cone momentum fraction carried by intrinsic heavy quarks in the proton $x_{Q\overline{Q}}$ as measured by the T^{++} component of the energy-momentum tensor is related in the heavy-quark limit to the forward matrix element $\langle p|\mathrm{tr}_c(G^{+\alpha}G^{+\beta}G_{\alpha\beta})/m_Q^2|p\rangle$, where $G^{\mu\nu}$ is the gauge field strength tensor. Diagrammatically, this can be described as a heavy quark loop in the proton self-energy with four gluons attached to the light, valence quarks. Since the non-Abelian commutator $[A_\alpha, A_\beta]$ is involved, the heavy

quark pairs in the proton wavefunction are necessarily in a color-octet state. It follows from dimensional analysis that the momentum fraction carried by the $Q\overline{Q}$ pair scales as $k_\perp^2/m_Q^2$ where $k_\perp$ is the typical momentum in the hadron wave function. [In contrast, in the case of Abelian theories, the contribution of an intrinsic, heavy lepton pair to the bound state's structure first appears in $O(1/m_L^4)$. One relevant operator corresponds to the Born-Infeld $(F_{\mu\nu})^4$ light-by-light scattering insertion, and the momentum fraction of heavy leptons in an atom scales as $k_\perp^4/m_L^4$.]

Intrinsic charm can be materialized by diffractive dissociation into open or hidden charm states such as $pp \to J/\psi X p', \Lambda_c X p'$. At HERA one can measure intrinsic charm in the proton by Coulomb dissociation: $pe \to \Lambda_C X e'$, and $J/\psi X e'$. Since the intrinsic heavy quarks tend to have the same rapidity as that of the projectile, they are produced at large x_F in the beam fragmentation region. The charm structure function measured by the EMC group shows an excess at large x_{bj}, indicating a probability of order 1% for intrinsic charm in the proton [19]. The presence of intrinsic charm in light-mesons provides an explanation for the puzzle of the large $J/\psi \to \rho\pi$ branching ratio and suppressed $\psi' \to \rho\pi$ decay [20]. The presence of intrinsic charm quarks in the B wave function provides new mechanisms for B decays. For example, Chang and Hou have considered the production of final states with three charmed quarks such as $B \to J/\psi D\pi$ and $B \to J/\psi D^*$ [21]; these final states are difficult to realize in the valence model, yet they occur naturally when the b quark of the intrinsic charm Fock state $|b\overline{u}c\overline{c}\rangle$ decays via $b \to c\overline{u}d$. In fact, the J/ψ spectrum for inclusive $B \to J/\psi X$ decays measured by CLEO and Belle shows a distinct enhancement at the low J/ψ momentum where such decays would kinematically occur. Alternatively, this excess could reflect the opening of baryonic channels such as $B \to J/\psi \overline{p}\Lambda$ [22]. Recently, Susan Gardner and I have shown that the presence of intrinsic charm in the hadrons' light-cone wave functions, even at a few percent level, provides new, competitive decay mechanisms for B decays which are nominally CKM-suppressed [23]. For example, the weak decays of the B-meson to two-body exclusive states consisting of strange plus light hadrons, such as $B \to \pi K$, are expected to be dominated by penguin contributions since the tree-level $b \to su\overline{u}$ decay is CKM suppressed. However, higher Fock states in the B wave function containing charm quark pairs can mediate the decay via a CKM-favored $b \to sc\overline{c}$ tree-level transition. Such intrinsic charm contributions can be phenomenologically significant. Since they mimic the amplitude structure of "charming" penguin contributions [24], charming penguins need not be penguins at all [23].

3 Calculating and Modeling Light-Cone Wavefunctions

The discretized light-cone quantization method [25] is a powerful technique for finding the non-perturbative solutions of quantum field theories. The basic method is to di-

agonalize the light-cone Hamiltonian in a light-cone Fock basis defined using periodic boundary conditions in x^- and $x_\perp$. The method preserves the frame-independence of the front form. The DLCQ method is now used extensively to solve one-space and one-time theories, including supersymmetric theories. New applications of DLCQ to supersymmetric quantum field theories and specific tests of the Maldacena conjecture have recently been given by Pinsky and Trittman. There has been progress in systematically developing the computation and renormalization methods needed to make DLCQ viable for QCD in physical spacetime. For example, John Hiller, Gary McCartor and I [26] have shown how DLCQ can be used to solve 3+1 theories despite the large numbers of degrees of freedom needed to enumerate the Fock basis. A key feature of our work, is the introduction of Pauli Villars fields in order to regulate the UV divergences and perform renormalization while preserving the frame-independence of the theory. A review of DLCQ and its applications is given in Ref. [27]. There has also been important progress using the transverse lattice, essentially a combination of DLCQ in 1+1 dimensions together with a lattice in the transverse dimensions.

Even without explicit solutions, many features of the light-cone wavefunctions follow from general arguments. Light-cone wavefunctions satisfy the equation of motion:

$$H_{LC}^{QCD}|\Psi\rangle = (H_{LC}^0 + V_{LC})|\Psi\rangle = M^2|\Psi\rangle,$$

which has the Heisenberg matrix form in Fock space:

$$M^2 - \sum_{i=1}^{n} \frac{m_{\perp i}^2}{x_i}\psi_n = \sum_{n'} \int \langle n|V|n'\rangle\, \psi_{n'}$$

where the convolution and sum is understood over the Fock number, transverse momenta, plus momenta and helicity of the intermediate states. Here $m_\perp^2 = m^2 + k_\perp^2$. Thus, in general, every light-cone Fock wavefunction has the form:

$$\psi_n = \frac{\Gamma_n}{M^2 - \sum_{i=1}^{n} \frac{m_{\perp i}^2}{x_i}}$$

where $\Gamma_n = \sum_{n'} \int V_{nn'}\psi_n$. The main dynamical dependence of a light-cone wavefunction away from the extrema is controlled by its light-cone energy denominator. The maximum of the wavefunction occurs when the invariant mass of the partons is minimal; *i.e.*, when all particles have equal rapidity and are all at rest in the rest frame. In fact, Dae Sung Hwang and I [28] have noted that one can rewrite the wavefunction in the form:

$$\psi_n = \frac{\Gamma_n}{M^2[\sum_{i=1}^{n} \frac{(x_i - \hat{x}_i)^2}{x_i} + \delta^2]}$$

where $x_i = \hat{x}_i \equiv m_{\perp i}/\sum_{i=1}^{n} m_{\perp i}$ is the condition for minimal rapidity differences of the constituents. The key parameter is $M^2 - \sum_{i=1}^{n} m_{\perp i}^2/\hat{x}_i \equiv -M^2\delta^2$. We can also interpret $\delta^2 \simeq 2\epsilon/M$ where $\epsilon = \sum_{i=1}^{n} m_{\perp i} - M$ is the effective binding energy. This

form shows that the wavefunction is a quadratic form around its maximum, and that the width of the distribution in $(x_i - \hat{x}_i)^2$ (where the wavefunction falls to half of its maximum) is controlled by $x_i\delta^2$ and the transverse momenta $k_{\perp_i}$. Note also that the heaviest particles tend to have the largest $\hat{x}_i$, and thus the largest momentum fraction of the particles in the Fock state, a feature familiar from the intrinsic charm model. For example, the b quark has the largest momentum fraction at small $k_\perp$ in the B meson's valence light-cone wavefunction,, but the distribution spreads out to an asymptotically symmetric distribution around $x_b \sim 1/2$ when $k_\perp >> m_b^2$.

We can also discern some general properties of the numerator of the light-cone wavefunctions. $\Gamma_n(x_i, k_{\perp i}, \lambda_i)$. The transverse momentum dependence of Γ_n guarantees J_z conservation for each Fock state: Each light-cone Fock wavefunction satisfies conservation of the z projection of angular momentum: $J^z = \sum_{i=1}^n S_i^z + \sum_{j=1}^{n-1} l_j^z$. The sum over s_i^z represents the contribution of the intrinsic spins of the n Fock state constituents. The sum over orbital angular momenta $l_j^z = -\mathrm{i}(k_j^1 \frac{\partial}{\partial k_j^2} - k_j^2 \frac{\partial}{\partial k_j^1})$ derives from the $n-1$ relative momenta. This excludes the contribution to the orbital angular momentum due to the motion of the center of mass, which is not an intrinsic property of the hadron [29]. For example, one of the three light-cone Fock wavefunctions of a $J_z = +1/2$ lepton in QED perturbation theory is $\psi^\uparrow_{+\frac{1}{2}+1}(x, \vec{k}_\perp) = -\sqrt{2}\frac{(-k^1+\mathrm{i}k^2)}{x(1-x)}\,\varphi$, where $\varphi = \varphi(x, \vec{k}_\perp) = \frac{e/\sqrt{1-x}}{M^2-(\vec{k}_\perp^2+m^2)/x-(\vec{k}_\perp^2+\lambda^2)/(1-x)}$. The orbital angular momentum projection in this case is $\ell^z = -1$. The spin structure indicated by perturbative theory provides a template for the numerator structure of the light-cone wavefunctions even for composite systems. The structure of the electron's Fock state in perturbative QED shows that it is natural to have a negative contribution from relative orbital angular momentum which balances the S_z of its photon constituents. We can also expect a significant orbital contribution to the proton's J_z since gluons carry roughly half of the proton's momentum, thus providing insight into the "spin crisis" in QCD.

The fall-off the light-cone wavefunctions at large $k_\perp$ and $x \to 1$ is dictated by QCD perturbation theory since the state is far-off the light-cone energy shell. This leads to counting rule behavior for the quark and gluon distributions at $x \to 1$. Notice that $x \to 1$ corresponds to $k^z \to -\infty$ for any constituent with nonzero mass or transverse momentum.

The above discussion suggests that an approximate form for the hadron light-cone wavefunctions might be constructed through variational principles and by minimizing the expectation value of H_{LC}^{QCD}.

4 Structure Functions are Not Parton Distributions

Ever since the earliest days of the parton model, it has been assumed that the leading-twist structure functions $F_i(x, Q^2)$ measured in deep inelastic lepton scattering are

determined by the *probability* distribution of quarks and gluons as determined by the light-cone wavefunctions of the target. For example, the quark distribution is

$$P_{q/N}(x_B, Q^2) = \sum_n \int^{k_{i\perp}^2 < Q^2} \left[\prod_i dx_i\, d^2k_{\perp i}\right] |\psi_n(x_i, k_{\perp i})|^2 \sum_{j=q} \delta(x_B - x_j).$$

The identification of structure functions with the square of light-cone wavefunctions is usually made in LC gauge $n \cdot A = A^+ = 0$, where the path-ordered exponential in the operator product for the forward virtual Compton amplitude apparently reduces to unity. Thus the deep inelastic lepton scattering cross section (DIS) appears to be fully determined by the probability distribution of partons in the target. However, Paul Hoyer, Nils Marchal, Stephane Peigne, Francesco Sannino, and I have recently shown that the leading-twist contribution to DIS is affected by diffractive rescattering of a quark in the target, a coherent effect which is not included in the light-cone wavefunctions, even in light-cone gauge. The distinction between structure functions and parton probabilities is already implied by the Glauber-Gribov picture of nuclear shadowing [30, 31, 32, 33]. In this framework shadowing arises from interference between complex rescattering amplitudes involving on-shell intermediate states, as in Fig. 1. In contrast, the wave function of a stable target is strictly real since it does not have on energy-shell configurations. A probabilistic interpretation of the DIS cross section is thus precluded.

It is well-known that in Feynman and other covariant gauges one has to evaluate the corrections to the "handbag" diagram due to the final state interactions of the struck quark (the line carrying momentum p_1 in Fig. 2) with the gauge field of the target. In light-cone gauge, this effect also involves rescattering of a spectator quark, the p_2 line in Fig. 2. The light-cone gauge is singular – in particular, the gluon propagator $d_{LC}^{\mu\nu}(k) = \frac{i}{k^2+i\varepsilon}\left[-g^{\mu\nu} + \frac{n^\mu k^\nu + k^\mu n^\nu}{n\cdot k}\right]$ has a pole at $k^+ = 0$ which requires an analytic prescription. In final-state scattering involving on-shell intermediate states, the exchanged momentum k^+ is of $O\left(1/\nu\right)$ in the target rest frame, which enhances the second term in the propagator. This enhancement allows rescattering to contribute at leading twist even in LC gauge.

The issues involving final state interactions even occur in the simple framework of abelian gauge theory with scalar quarks. Consider a frame with $q^+ < 0$. We can then distinguish FSI from ISI using LC time-ordered perturbation theory [13]. Figure 1 illustrates two LCPTH diagrams which contribute to the forward $\gamma^* T \to \gamma^* T$ amplitude, where the target T is taken to be a single quark. In the aligned jet kinematics the virtual photon fluctuates into a $q\overline{q}$ pair with limited transverse momentum, and the (struck) quark takes nearly all the longitudinal momentum of the photon. The initial q and $\overline{q}$ momenta are denoted p_1 and $p_2 - k_1$, respectively,

The calculation of the rescattering effect of DIS in Feynman and light-cone gauge through three loops is given in detail in Ref. [34]. The result can be resummed and is most easily expressed in eikonal form in terms of transverse distances $r_\perp, R_\perp$

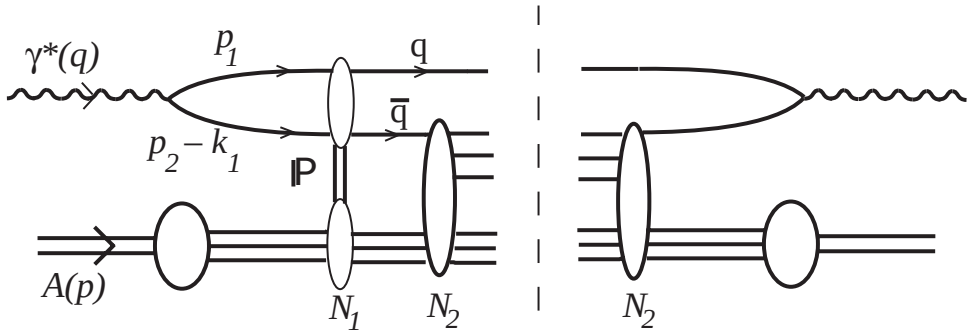

Figure 1: Glauber-Gribov shadowing involves interference between rescattering amplitudes.

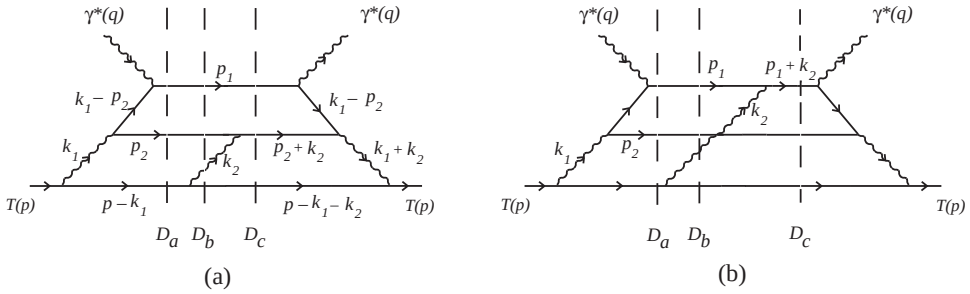

Figure 2: Two types of final state interactions. (a) Scattering of the antiquark (p_2 line), which in the aligned jet kinematics is part of the target dynamics. (b) Scattering of the current quark (p_1 line). For each LC time-ordered diagram, the potentially on-shell intermediate states – corresponding to the zeroes of the denominators D_a, D_b, D_c – are denoted by dashed lines.

conjugate to $p_{2\perp}, k_\perp$. The deep inelastic cross section can be expressed as

$$Q^4 \frac{d\sigma}{dQ^2\, dx_B} = \frac{\alpha}{16\pi^2} \frac{1-y}{y^2} \frac{1}{2M\nu} \int \frac{dp_2^-}{p_2^-}\, d^2\vec{r}_\perp\, d^2\vec{R}_\perp\, |\tilde{M}|^2 \tag{1}$$

where

$$|\tilde{M}(p_2^-, \vec{r}_\perp, \vec{R}_\perp)| = \left| \frac{\sin\left[g^2\, W(\vec{r}_\perp, \vec{R}_\perp)/2\right]}{g^2\, W(\vec{r}_\perp, \vec{R}_\perp)/2} \tilde{A}(p_2^-, \vec{r}_\perp, \vec{R}_\perp) \right| \tag{2}$$

is the resummed result. The Born amplitude is

$$\tilde{A}(p_2^-, \vec{r}_\perp, \vec{R}_\perp) = 2eg^2 MQ p_2^-\, V(m_{||} r_\perp) W(\vec{r}_\perp, \vec{R}_\perp) \tag{3}$$

where $m_{||}^2 = p_2^- M x_B + m^2$ and

$$V(m\, r_\perp) \equiv \int \frac{d^2\vec{p}_\perp}{(2\pi)^2} \frac{e^{i\vec{r}_\perp \cdot \vec{p}_\perp}}{p_\perp^2 + m^2} = \frac{1}{2\pi} K_0(m\, r_\perp) \tag{4}$$

The rescattering effect of the dipole of the $q\overline{q}$ is controlled by

$$W(\vec{r}_\perp, \vec{R}_\perp) \equiv \int \frac{d^2\vec{k}_\perp}{(2\pi)^2} \frac{1 - e^{i\vec{r}_\perp \cdot \vec{k}_\perp}}{k_\perp^2} e^{i\vec{R}_\perp \cdot \vec{k}_\perp} = \frac{1}{2\pi} \log\left(\frac{|\vec{R}_\perp + \vec{r}_\perp|}{R_\perp}\right). \tag{5}$$

The fact that the coefficient of $\tilde{A}$ in (2) is less than unity for all $\vec{r}_\perp, \vec{R}_\perp$ shows that the rescattering corrections reduce the cross section. It is the analog of nuclear shadowing in our model.

We have also found the same result for the deep inelastic cross sections in light-cone gauge. Three prescriptions for defining the propagator pole at $k^+ = 0$ have been used in the literature:

$$\frac{1}{k_i^+} \to \left[\frac{1}{k_i^+}\right]_{\eta_i} = \begin{cases} k_i^+ \left[(k_i^+ - i\eta_i)(k_i^+ + i\eta_i)\right]^{-1} & \text{(PV)} \\ \left[k_i^+ - i\eta_i\right]^{-1} & \text{(K)} \\ \left[k_i^+ - i\eta_i \epsilon(k_i^-)\right]^{-1} & \text{(ML)} \end{cases} \tag{6}$$

the principal-value, Kovchegov [35], and Mandelstam-Leibbrandt [36] prescriptions. The 'sign function' is denoted $\epsilon(x) = \Theta(x) - \Theta(-x)$. With the PV prescription we have $I_\eta = \int dk_2^+ \left[\frac{1}{k_2^+}\right]_{\eta_2} = 0$. Since an individual diagram may contain pole terms $\sim 1/k_i^+$, its value can depend on the prescription used for light-cone gauge. However, the $k_i^+ = 0$ poles cancel when all diagrams are added; the net is thus prescription-independent, and it agrees with the Feynman gauge result. It is interesting to note that the diagrams involving rescattering of the struck quark p_1 do not contribute to the leading-twist structure functions if we use the Kovchegov prescription to define the light-cone gauge. In other prescriptions for light-cone gauge the rescattering of the struck quark line p_1 leads to an infrared divergent phase factor $\exp i\phi$:

$$\phi = g^2 \, \frac{I_\eta - 1}{4\pi} \, K_0(\lambda R_\perp) + O(g^6) \tag{7}$$

where λ is an infrared regulator, and $I_\eta = 1$ in the K prescription. The phase is exactly compensated by an equal and opposite phase from final-state interactions of line p_2. This irrelevant change of phase can be understood by the fact that the different prescriptions are related by a residual gauge transformation proportional to $\delta(k^+)$ which leaves the light-cone gauge $A^+ = 0$ condition unaffected.

Diffractive contributions which leave the target intact thus contribute at leading twist to deep inelastic scattering. These contributions do not resolve the quark structure of the target, and thus they are contributions to structure functions which are not parton probabilities. More generally, the rescattering contributions shadow and modify the observed inelastic contributions to DIS.

Our analysis in the K prescription for light-cone gauge resembles the "covariant parton model" of Landshoff, Polkinghorne and Short [37, 38] when interpreted in

the target rest frame. In this description of small x DIS, the virtual photon with positive q^+ first splits into the pair p_1 and p_2. The aligned quark p_1 has no final state interactions. However, the antiquark line p_2 can interact in the target with an effective energy $\hat{s} \propto k_\perp^2/x$ while staying close to its mass shell. Thus at small x and large $\hat{s}$, the antiquark p_2 line can first multiple scatter in the target via pomeron and Reggeon exchange, and then it can finally scatter inelastically or be annihilated. The DIS cross section can thus be written as an integral of the $\sigma_{\overline{q}p\to X}$ cross section over the p_2 virtuality. In this way, the shadowing of the antiquark in the nucleus $\sigma_{\overline{q}A\to X}$ cross section yields the nuclear shadowing of DIS [32]. Our analysis, when interpreted in frames with $q^+ > 0$, also supports the color dipole description of deep inelastic lepton scattering at small x. Even in the case of the aligned jet configurations, one can understand DIS as due to the coherent color gauge interactions of the incoming quark-pair state of the photon interacting first coherently and finally incoherently in the target.

5 Acknowledgment

I thank Professor Vojtech Kundrat for organizing this outstanding meeting. Much of the new work reported here was done in collaboration with others, especially, Susan Gardner, Dae Sung Hwang, Paul Hoyer, Nils Marchal, Stephane Peigne, and Francesco Sannino. This work was supported by the Department of Energy under contract number DE-AC03-76SF00515.

References

[1] S. J. Brodsky and D. S. Hwang, Nucl. Phys. B **543**, 239 (1999) [hep-ph/9806358].

[2] S. J. Brodsky, V. S. Fadin, V. T. Kim, L. N. Lipatov and G. B. Pivovarov, JETP Lett. **70**, 155 (1999) [hep-ph/9901229].

[3] A. Donnachie and P. V. Landshoff, hep-ph/0105088.

[4] S. J. Brodsky and D.-S. Hwang, in preparation.

[5] S. J. Brodsky and A. H. Mueller, Phys. Lett. B **206**, 685 (1988).

[6] G. Bertsch, S. J. Brodsky, A. S. Goldhaber and J. F. Gunion, Phys. Rev. Lett. **47**, 297 (1981).

[7] S. Brodsky, P.Hoyer, Markus Diehl, S. Peigne, and W. Schäfer, (in preparation).

[8] L. Frankfurt, G. A. Miller and M. Strikman, Phys. Lett. B **304**, 1 (1993) [hep-ph/9305228].

[9] L. Frankfurt, G. A. Miller and M. Strikman, hep-ph/0010297.

[10] E. M. Aitala *et al.* [E791 Collaboration], Phys. Rev. Lett. **86**, 4773 (2001) [hep-ex/0010044].

[11] E. M. Aitala *et al.* [E791 Collaboration], Phys. Rev. Lett. **86**, 4768 (2001) [hep-ex/0010043].

[12] J. Gronberg *et al.* [CLEO Collaboration], Phys. Rev. D **57**, 33 (1998) [hep-ex/9707031].

[13] G. P. Lepage and S. J. Brodsky, Phys. Rev. D **22**, 2157 (1980).

[14] V. M. Braun, D. Y. Ivanov, A. Schafer and L. Szymanowski, *Phys. Lett. B* **509**, 43 (2001) [hep-ph/0103275].

[15] V. Chernyak, [hep-ph/0103295].

[16] G. A. Miller, Int. J. Mod. Phys. B **15**, 1551 (2001) [nucl-th/9910053].

[17] G. A. Miller, S. J. Brodsky and M. Karliner, Phys. Lett. B **481**, 245 (2000) [hep-ph/0002156].

[18] M. Franz, V. Polyakov and K. Goeke, Phys. Rev. D **62**, 074024 (2000) [hep-ph/0002240].

[19] B. W. Harris, J. Smith and R. Vogt, Nucl. Phys. B **461**, 181 (1996) [hep-ph/9508403].

[20] S. J. Brodsky and M. Karliner, Phys. Rev. Lett. **78**, 4682 (1997) [hep-ph/9704379].

[21] C. V. Chang and W. Hou, hep-ph/0101162.

[22] S. J. Brodsky and F. S. Navarra, Phys. Lett. B **411**, 152 (1997) [hep-ph/9704348].

[23] S. J. Brodsky and S. Gardner, hep-ph/0108121.

[24] M. Ciuchini, E. Franco, G. Martinelli, M. Pierini and L. Silvestrini, Phys. Lett. B **515**, 33 (2001) [hep-ph/0104126].

[25] H. C. Pauli and S. J. Brodsky, Phys. Rev. D **32**, 1993 (1985).

[26] S. J. Brodsky, J. R. Hiller and G. McCartor, hep-ph/0107038.

[27] S. J. Brodsky, H. Pauli and S. S. Pinsky, Phys. Rept. **301**, 299 (1998) [hep-ph/9705477].

[28] S. J. Brodsky and D. S. Hwang, in preparation.

[29] S. J. Brodsky, D. S. Hwang, B. Ma and I. Schmidt, Nucl. Phys. B **593**, 311 (2001) [hep-th/0003082].

[30] V. N. Gribov, Sov. Phys. JETP **29**, 483 (1969) [Zh. Eksp. Teor. Fiz. **56**, 892 (1969)].

[31] S. J. Brodsky and J. Pumplin, Phys. Rev. **182**, 1794 (1969).

[32] S. J. Brodsky and H. J. Lu, Phys. Rev. Lett. **64**, 1342 (1990).

[33] G. Piller and W. Weise, Phys. Rept. **330**, 1 (2000) [hep-ph/9908230].

[34] S. J. Brodsky, P. Hoyer, N. Marchal, S. Peigne and F. Sannino, hep-ph/0104291.

[35] Y. V. Kovchegov, Phys. Rev. D **55**, 5445 (1997) [hep-ph/9701229].

[36] G. Leibbrandt, Rev. Mod. Phys. **59**, 1067 (1987).

[37] P. V. Landshoff, J. C. Polkinghorne and R. D. Short, Nucl. Phys. B **28**, 225 (1971).

[38] S. J. Brodsky, F. E. Close and J. F. Gunion, Phys. Rev. D **8**, 3678 (1973).